ORBIT IMPROVEMENT FROM SATELLITE IMAGING DATA OBTAINABLE FROM THE MARINER/JUPITER/SATURN 1977 MISSIONS

Final Report

Grant NGR 09-015-184

Principal Investigator
Dr. Kaare Aksnes

July 1972

Prepared for

National Aeronautics and Space Administration
Washington, D.C. 20546

Smithsonian Institution
Astrophysical Observatory
Cambridge, Massachusetts 02138

ORBIT IMPROVEMENT FROM SATELLITE IMAGING DATA OBTAINABLE FROM THE MARINER/JUPITER/SATURN 1977 MISSIONS

Final Report

Grant NGR 09-015-184

Principal Investigator
Dr. Kaare Aksnes

July 1972

Prepared for

National Aeronautics and Space Administration
Washington, D.C. 20546

Smithsonian Institution
Astrophysical Observatory
Cambridge, Massachusetts 02138

207-070

ORBIT IMPROVEMENT FROM SATELLITE IMAGING DATA OBTAINABLE FROM MARINER/JUPITER/SATURN 1977 MISSIONS

Kaare Aksnes

Smithsonian Astrophysical Observatory, Cambridge, Mass. 02138, U.S.A.

Abstract. Equations of motion are established for a dynamical system in which a spacecraft flies close to and interacts with an outer planet and one or more of its satellites. For the computation of the state and mass partials ($\partial \bar{r}_i / \partial \bar{r}_{j0}$ and $\partial \bar{r}_i / \partial m_j$) needed in the orbit corrections, a set of variational equations is derived. These assume a notably compact form through the introduction of a matrix operator D. The above system of differential equations is integrated numerically on a computer.

Spacecraft-satellite direction measurements accurate to $\pm 10''$ were simulated along three representative Mariner/Jupiter/Saturn trajectories approaching Io, Titan, and Iapetus to within 41,000, 13,000, and 7,000 km, respectively. For example, from measurements distributed evenly at half-day intervals over a 60-day arc centered on encounter, but none so close that the satellite would fill more than 0.5° in the sky, the orbit of the satellite and that of the spacecraft can be estimated to about 100 km. In addition, the mass of the satellite is obtainable to 2.6% for Io, 1.4% for Titan, and 9% for Iapetus. If only measurements up to 3 days before satellite encounter are included, the orbit of the satellite or that of the spacecraft can be estimated to about 300 km, all information on mass being lost.

1. Introduction

The Mariner/Jupiter/Saturn (MJS) 1977 missions will encounter several natural satellites. The goal of this study has been to determine the potential value of spacecraft-centered TV-imaging data on these satellites for improving the ephemerides of the satellites and for aiding the navigation of the spacecraft in their vicinity. More specifically, we seek answers to the following questions:

1) On the basis of simulated satellite imaging data, how large are the improvements we can expect in the values of (a) the orbital parameters of the satellites and of the spacecraft, (b) the masses of the satellites, and (c) the masses and zonal-harmonic coefficients of the primaries?

2) In order to maximize the return of information for question 1), how should spacecraft trajectories be chosen and the observations be distributed along them?

The power of TV-imaging data of satellites to improve ephemerides has already been demonstrated (Born and Duxbury, 1972) for Mars' satellites Phobos and Deimos, which were photographed from the Mariner 9 spacecraft/orbiter last year. It was estimated that whenever, on a TV frame, stars were visible together with one of the satellites, the latter's position could be measured to an accuracy of about 5". This made it possible to estimate the positions of Mars' satellites to better than 10 km. These results are very encouraging, but a direct extrapolation to the satellites of the outer planets must be cautioned against. Even if we exclude satellite imaging data from the Mariner 9 orbiter phase, which will have no counterpart on a MJS mission, there remain significant differences between the two with regard to the satellite data and their use: The latter mission is characterized by approach velocities approximately 10 times greater; the data must be taken at much greater distances; and the target satellites are hundreds of times larger. While a relatively simple analytic satellite theory (Aksnes, 1972) was sufficient for analyzing the data on Phobos and Deimos, the satellites of Jupiter and Saturn present a much more complicated dynamical problem owing to mass interactions between them and the spacecraft. This

circumstance should be welcomed because the deflection of the spacecraft caused by a nearby satellite promises to yield a strong determination of its mass. It does mean, however, that a numerical integration of the equations of motion and their variational equations is the only technique available. Although demanding in computer time, this numerical approach is feasible because time intervals of only a few months at each planet are involved.

2. The Dynamical Model

2.1 Equations of motion

For our purpose, we assume that a massless spacecraft (or an orbiter) is moving under the attractions of an oblate planet and n-1 gravitationally interacting satellites, each treated as a point mass. In Figure 1, m_0 denotes the mass of the planet, and m_i and r_i are the mass and the planetocentric position vector, respectively, of the i-th body, i being 1 for the spacecraft and $2, 3, \ldots, n$ for the satellites. The equations of motion then take the form

$$\frac{d^2\bar{r}_i}{dt^2} + (\mu_0 + \mu_i)\frac{\bar{r}_i}{r_i^3} = \sum_{\substack{j=1 \\ j\neq i}}^{n} \mu_j \left(\frac{\bar{r}_j - \bar{r}_i}{r_{ji}^3} - \frac{\bar{r}_j}{r_j^3} \right) + \nabla_i R_i \ , \qquad i = 1, 2, \ldots, n \ , \quad (1)$$

where μ_i denotes the product of the gravitational constant and m_i, and where r_{ji} is the distance between the i-th and j-th bodies. Furthermore, $\nabla_i R_i$ denotes the gradient, with respect to the cartesian coordinates x_i, y_i, z_i, of the i-th body, of the disturbing function

$$R_i = -\mu_0 \sum_{k=2}^{\infty} J_k \frac{R^k}{r_i^{k+1}} P_k(\sin \theta_i) \ . \quad (2)$$

Here, R will be recognized as the equatorial radius of the planet, θ_i as the latitude of the i-th body above the planet's equatorial plane, and J_k as the coefficient of the k-th zonal harmonic.

Let us now assume that the coordinates are referred to the Earth's mean equator and equinox of 1950.0. To express $\sin \theta_i$ in terms of x_i, y_i, z_i, we introduce the right ascension α and the declination δ of the planet's north pole. We then define a planet equatorial system by rotating the xyz-system $\alpha + 90°$ about the z-axis, and $90° - \delta$ about the x-axis. Hence,

$$\begin{bmatrix} x' \\ y' \\ z' \end{bmatrix} = \begin{bmatrix} -\sin \alpha & , & \cos \alpha & , & 0 \\ -\cos \alpha \sin \delta & , & -\sin \alpha \sin \delta & , & \cos \delta \\ \cos \alpha \cos \delta & , & \sin \alpha \cos \delta & , & \sin \delta \end{bmatrix} \begin{bmatrix} x \\ y \\ z \end{bmatrix} , \tag{3}$$

from which transformation it follows that

$$r_i \sin \theta_i = z_i' = \cos \alpha \cos \delta \cdot x_i + \sin \alpha \cos \delta \cdot y_i + \sin \delta \cdot z_i \quad . \tag{4}$$

Then,

$$\nabla_i R_i = \begin{bmatrix} x_i/r_i & , & \partial \sin \theta_i/\partial x_i \\ y_i/r_i & , & \partial \sin \theta_i/\partial y_i \\ z_i/r_i & , & \partial \sin \theta_i/\partial z_i \end{bmatrix} \begin{bmatrix} \partial R_i/\partial r_i \\ \partial R_i/\partial \sin \theta_i \end{bmatrix} . \tag{5}$$

In the Explanatory Supplement to the Ephemeris, the quantities α and δ for the planets are given as slowly varying linear functions of time. For simplicity, we assume in our simulation study that α and δ are constant during the short planetary-flyby periods, and the coordinates will be referred to the equatorial planes of the planets by making $\alpha = 0°$ and $\delta = 90°$. Equation (5) can then be written

$$\nabla_i R_i = \begin{bmatrix} x_i & , & -x_i z_i/r_i^2 \\ y_i & , & -y_i z_i/r_i^2 \\ z_i & , & -z_i^2/r_i^2 + 1 \end{bmatrix} \begin{bmatrix} \mu_0 \sum_{k=2}^{\infty} J_k (k+1) R^k P_k(\sin \theta_i)/r_i^{k+3} \\ -\mu_0 \sum_{k=2}^{\infty} J_k R^k P_k'(\sin \theta_i)/r_i^{k+2} \end{bmatrix} . \tag{6}$$

2.2 Variational equations

Let a solution of the equations of motion (1) be expressed symbolically as

$$\bar{r}_i = \bar{r}_i(P_1, P_2, \ldots, P_n; p_1, p_2, \ldots, p_m, t) \quad , \qquad i = 1, 2, \ldots, n \quad , \tag{7}$$

where P_j $(j = 1, 2, \ldots, n)$ is the column vector $\{x_{j0}, y_{j0}, z_{j0}, \dot{x}_{j0}, \dot{y}_{j0}, \dot{z}_{j0}\}$ defining the initial position and velocity of the j-th body, while $p_1, p_2, \ldots, p_m$ denote m scalar parameters, e.g., satellite masses and zonal-harmonic coefficients. By varying the arguments of $\bar{r}_i$, we obtain

$$\begin{bmatrix} \delta\bar{r}_1 \\ \delta\bar{r}_2 \\ - \\ \delta\bar{r}_n \end{bmatrix} = \begin{bmatrix} G_{11}, \ldots, G_{1n} \\ - \quad - \\ - \quad - \\ G_{n1}, \ldots, G_{nn} \end{bmatrix} \begin{bmatrix} \delta P_1 \\ \delta P_2 \\ - \\ \delta P_n \end{bmatrix} + \begin{bmatrix} g_{11}, \ldots, g_{1m} \\ - \quad - \\ - \quad - \\ g_{n1}, \ldots, g_{nm} \end{bmatrix} \begin{bmatrix} \delta p_1 \\ \delta p_2 \\ - \\ \delta p_n \end{bmatrix}$$

or, in matrix form,

$$\delta\bar{r} = G \cdot \delta P + g \cdot \delta p \quad . \tag{8}$$

Here, G and g are $n \times n$ and $n \times m$ matrices whose elements G_{ij} and g_{ik} are, in turn, the 3×6 and 3×1 matrices given by

$$G_{ij} = \frac{\partial \bar{r}_i}{\partial \bar{r}_j} = \begin{bmatrix} \frac{\partial x_i}{\partial x_{j0}}, \frac{\partial x_i}{\partial y_{j0}}, \cdots, \frac{\partial x_i}{\partial \dot{z}_{j0}} \\ \frac{\partial y_i}{\partial x_{j0}}, \frac{\partial y_i}{\partial y_{j0}}, \cdots, \frac{\partial y_i}{\partial \dot{z}_{j0}} \\ \frac{\partial z_i}{\partial x_{j0}}, \frac{\partial z_i}{\partial y_{j0}}, \cdots, \frac{\partial z_i}{\partial \dot{z}_{j0}} \end{bmatrix} \quad ; \qquad g_{ik} = \frac{\partial \bar{r}_i}{\partial p_k} = \begin{bmatrix} \frac{\partial x_i}{\partial p_k} \\ \frac{\partial y_i}{\partial p_k} \\ \frac{\partial z_i}{\partial p_k} \end{bmatrix} \quad , \tag{9}$$

where i and $j = 1, 2, \ldots, n$ and $k = 1, 2, \ldots, m$. If we interpret $\delta\bar{r}$ as the difference between observed and computed values of $\bar{r}$, then (8) becomes an equation of condition. From a series of observations, corrections δP and δp to the nominal values of the

constant parameters P and p can be found by the method of least squares, provided that the coefficients G and g can be computed. To this end, we differentiate Equations (9) twice with respect to t:

$$\ddot{G}_{ij} = \frac{\partial \ddot{\bar{r}}_i}{\partial P_j} = \sum_{\ell=1}^{n} \frac{\partial \ddot{\bar{r}}_i}{\partial \bar{r}_\ell} \frac{\partial \bar{r}_\ell}{\partial P_j} ,$$

$$\ddot{g}_{ik} = \frac{\partial \ddot{\bar{r}}_i}{\partial p_k} = \sum_{\ell=1}^{n} \frac{\partial \ddot{\bar{r}}_i}{\partial \bar{r}_\ell} \frac{\partial \bar{r}_\ell}{\partial p_k} + \frac{\partial \ddot{\bar{r}}_i}{\partial p_k} ,$$

where the terms under the summation signs are due to the implicit dependence of $\ddot{\bar{r}}_i$ in (1) on P_j and p_k, while the last term arises because of the explicit dependence on p_k. For the determination of G_{ij} and g_{ik}, we thus arrive at the differential equations (variational equations),

$$\ddot{G}_{ij} = \sum_{\ell=1}^{n} \frac{\partial \ddot{\bar{r}}_i}{\partial \bar{r}_\ell} G_{\ell j} , \qquad i, j = 1, 2, \ldots, n ,$$

$$\ddot{g}_{ik} = \sum_{\ell=1}^{n} \frac{\partial \ddot{\bar{r}}_i}{\partial \bar{r}_\ell} g_{\ell k} + \frac{\partial \ddot{\bar{r}}_i}{\partial p_k} , \qquad k = 1, 2, \ldots, n , \tag{10}$$

with initial conditions,

$$G_{ij} = \begin{bmatrix} 1 & 0 & 0 & 0 & 0 & 0 \\ 0 & 1 & 0 & 0 & 0 & 0 \\ 0 & 0 & 1 & 0 & 0 & 0 \end{bmatrix} \delta_{ij} , \quad \dot{G}_{ij} = \begin{bmatrix} 0 & 0 & 0 & 1 & 0 & 0 \\ 0 & 0 & 0 & 0 & 1 & 0 \\ 0 & 0 & 0 & 0 & 0 & 1 \end{bmatrix} \delta_{ij} ;$$

$$g_{ik} = \dot{g}_{ik} = \begin{bmatrix} 0 \\ 0 \\ 0 \end{bmatrix} , \qquad \delta_{ij} = \begin{cases} 1 & \text{for } i = j \\ 0 & \text{for } i \neq j \end{cases} . \tag{11}$$

To derive expressions for the partial derivatives in Equations (10), we vary both sides of Equation (1):

$$\delta\ddot{\bar{r}}_i = -\delta(\mu_0 + \mu_i)\frac{\bar{r}_i}{r_i^3} + \sum_j \delta\mu_j\left(\frac{\bar{r}_j - \bar{r}_i}{r_{ji}^3} - \frac{\bar{r}_j}{r_j^3}\right) + (\mu_0 + \mu_i)\, D(\bar{r}_i)\, \delta\bar{r}_i$$

$$+ \sum_j \mu_j\, D(\bar{r}_j)\, \delta\bar{r}_j - \sum_j \mu_j\, D(\bar{r}_j - \bar{r}_i)\, \delta(\bar{r}_j - \bar{r}_i) + \nabla_i \delta R_i \ , \qquad (12)$$

where D is a matrix operator defined in terms of a vector $\bar{r} = [x, y, z]$ and the identity matrix I as follows:

$$D(\bar{r}) = \frac{1}{r^3}\left[\frac{3\bar{r}\bar{r}}{r^2} - I\right] = \frac{3}{r^5}\begin{bmatrix} x^2 - r^2/3 & xy & xz \\ yx & y^2 - r^2/3 & yz \\ zx & zy & z^2 - r^2/3 \end{bmatrix} . \qquad (13)$$

In Equation (12), R_i is to be varied only with respect to the quantity $\mu_0 R^k J_k$ in Equation (2). Thus, we neglect terms of the type $J_k \delta\bar{r}_i$, which should contribute only negligibly during the short time intervals considered here. The terms factored by the central mass μ_0 will of course dominate, except that if r_{ji} should become very small during a close approach to a satellite, the corresponding term will be brought into sudden prominence. We now immediately deduce

$$\frac{\partial\ddot{\bar{r}}_i}{\partial\bar{r}_j} = \mu_j\, D(\bar{r}_j) - \mu_j\, D(\bar{r}_j - \bar{r}_i) \ ,$$

$$\frac{\partial\ddot{\bar{r}}_i}{\partial\bar{r}_i} = (\mu_0 + \mu_i)\, D(\bar{r}_i) + \sum_{\substack{\ell=1 \\ \ell\neq i}}^{n} \mu_\ell\, D(\bar{r}_\ell - \bar{r}_i) \ , \qquad (14)$$

$$\frac{\partial\ddot{\bar{r}}_i}{\partial\mu_0} = \frac{\partial\ddot{\bar{r}}_i}{\partial\mu_i} = -\frac{\bar{r}_i}{r_i^3} \ , \qquad \frac{\partial\ddot{\bar{r}}_i}{\partial\mu_j} = \frac{\bar{r}_j - \bar{r}_i}{r_{ji}^3} - \frac{\bar{r}_j}{r_j^3} \ ,$$

(continued)

$$\frac{\partial \ddot{\bar{r}}_i}{\partial(\mu_0 R^k J_k)} = \begin{bmatrix} x_i\,, & -x_i z_i / r_i^2 \\ y_i\,, & -y_i z_i / r_i^2 \\ z_i\,, & -z_i^2 / r_i^2 + 1 \end{bmatrix} \begin{bmatrix} (k+1)\, P_k(\sin\theta_i) / r_i^{k+3} \\ -P_k'(\sin\theta_i) / r_i^{k+2} \end{bmatrix} ,$$

where $i, j\ (i \neq j) = 1, 2, \ldots, n$, $k = 2, 3, \ldots, \infty$; P_k, the Legendre polynomial of order k, should not be confused with the parameters P_k introduced in Equation (7).

3. Numerical Results

Based on the equations established in the preceding section, a computer program has been developed that can differentially correct the following 17 parameters:

$P_1 = [x_{10}, y_{10}, z_{10}, \dot{x}_{10}, \dot{y}_{10}, \dot{z}_{10}]$, initial conditions of spacecraft;

$P_2 = [x_{20}, y_{20}, z_{20}, \dot{x}_{20}, \dot{y}_{20}, \dot{z}_{20}]$, initial conditions of satellite;

$p_1 = \mu_2$, mass of satellite;

$p_2 = \mu_0$, mass of primary;

$p_3, p_4, p_5 = J_2, J_3, J_4$, form factors of primary.

For simplicity, we have assumed that the satellite under consideration is body number 2. Although we have limited the number of bodies to three (primary, satellite, and spacecraft) in our simulation runs, the program will accept an arbitrary number of perturbing bodies, which need not be only satellites. If we were dealing with actual imaging data, such additional bodies would, of course, have to be included. However, they would only complicate our simulation without adding much new insight.

Our equation of condition (8) now becomes

$$\delta\bar{r} = \sum_{i=1}^{2} (G_{2i} - G_{1i})\ \delta P_i + \sum_{k=1}^{5} (g_{2k} - g_{1k})\ \delta p_k \ , \qquad (15)$$

where the G's, g's, and $\delta\bar{r}$, i.e., the difference between the "observed" and the computed values of $\bar{r} = \bar{r}_2 - \bar{r}_1$, are obtained by numerical integration of Equations (1) and (10) by means of (14). Note that since the spacecraft has no effect on the satellite, $\partial\bar{r}_2/\partial\bar{r}_1 = G_{21} = 0$. In practice, we will be dealing with direction measurements – say, longitude φ and latitude θ in the planet-equatorial xyz-system. Equation (15) must then be modified to

$$\begin{bmatrix} \cos\theta\delta\varphi \\ \delta\theta \end{bmatrix} = \begin{bmatrix} -\sin\varphi & , & \cos\varphi & , & 0 \\ -\sin\theta\cos\varphi, & & -\sin\theta\sin\varphi, & & \cos\theta \end{bmatrix} \frac{\delta\bar{r}}{r} . \qquad (16)$$

We have used this program to analyze three representative MJS trajectories (Burke et al., 1972) approaching Io, Titan, and Iapetus to within about 41,000 13,000, and 7,000 km, respectively. The corresponding initial conditions, in the form of nominal values of the above-mentioned 17 parameters, were used to generate fictitious spacecraft/satellite direction measurements with the distributions shown in Table I. The table also gives the times of encounter with the planets (E) and with the satellites, and the associated minimum ranges (Δ) to the center of each body. Finally, for each case, the range and time of the closest observations are given. The observations are distributed evenly within the indicated time intervals, except for a few observations dropped because of the imposition of a cutoff value on the satellite range. Note that in the first two cases of each flyby, the observations are grouped fairly symmetrically about the satellite encounters. As will be demonstrated later, it is also important to observe the satellites after encounter. They will then appear much fainter than before encounter because of the large phase angles ($> 100°$) under which they will be seen. Since it is difficult to record very bright satellites and faint reference stars simultaneously, the reduced satellite brightness after encounter should actually be an advantage.

It is perhaps unrealistic to hope to obtain precise astrometric data of the satellites when they fill more than $0.5°$ of the field of view of the camera. This occurs at distances below roughly 400,000, 560,000, and 150,000 km from Io, Titan, and Iapetus, respectively. For this reason, and also because of the high observation frequency near encounter (~ 2 observations/hr), Cases 1 for the former two satellites

are probably not realistic. Case 1 for Iapetus may be more indicative of what can be achieved in practice. There, observations for which the angular diameter of the satellite exceeds 0.5° are excluded, the shortest observation interval being 3 hr. The observations are now spread out over 60 instead of 10 days, although one-half of the observations are concentrated in 1 week around encounter. In Cases 2 for all three satellites, the imaging requirements are relaxed even further by distributing the observations evenly over the entire 60-day arc at half-day intervals.

Cases 3 and 4 should be representative for the imaging data that would be available for navigating the spacecraft and aiding camera pointing during the satellite flybys. Excluded from Cases 3 and 4 are observations obtained later than about 1 and 3 days, respectively, before the satellite encounters in order to allow time for transmitting the observations to Earth, performing the orbit corrections, and transmitting the necessary commands back to the spacecraft.

To simulate noise, a random error within the limits $\pm 10''$, which is compatible with the capability of the baseline MJS imaging system, was added to each observation. Finally, before the program for each of the cases listed in Table II was run, the parameters to be corrected were contaminated with errors of 1000 km and 0.01 km/s in the position and velocity components, and 10% in the other parameters. Table II gives for the corrected parameters the standard errors resulting from the least-squares fits, together with their actual errors, i.e., the deviations from the nominal values. It is reassuring to observe that these two types of errors are in reasonable agreement. Interestingly enough, probable errors, defined as 0.67 times the standard errors, would fit the actual errors considerably better in most cases. To the extent that the observation errors are truely random, the standard errors should be proportional to the average observation error (this was actually verified by rerunning Case 1 for Io with observation errors between $\pm 20''$ instead of $\pm 10''$) and to the inverse square root of the number of observations.

4. Conclusions

On the basis of Table II and a few cases not reported there, the following answers to the questions raised in the Introduction have evolved:

1a) The MJS satellite imaging data (Cases 1 and 2) should make it possible to estimate, for a period of a few months, the positions of Io, Titan, Iapetus, and the spacecraft to within several tens to several hundreds of kilometers, depending on the distribution of the data and on the satellite. The corresponding velocity errors vary from a fraction of a meter per second to a few meters per second. Comparable results can be expected for other satellites that the spacecraft approaches to within, say, one million kilometers. Even better results are possible by utilizing the radio tracking data of the spacecraft in addition to the imaging data. If the observations after encounter are excluded (Cases 3 and 4), the position components of the satellite become rather strongly correlated with those of the spacecraft. However, if the latter parameters are assumed to be known well enough from the radio tracking data, the imaging data suffice for improving the ephemeris of the satellite to a few hundred kilometers (Cases 3c and 4). This is probably sufficient for navigation purposes.

The seriousness of the problem of camera pointing is illustrated rather dramatically during the close passage of, for example, Titan in Case 1: At the epoch (Saturn encounter), the induced position and velocity errors of the spacecraft relative to Titan amount to a few thousand kilometers and a few tens of meters per second. These errors are rather smaller than what can be expected in practice. Nevertheless, they cause an impressive 17° displacement of Titan as seen from the spacecraft at a distance of 14,000 km. After orbit correction, which in this case needed many iterations before converging, this displacement was reduced to 0.003°! Although, as explained earlier, the distribution of the observations is undoubtedly too optimistic in this case, it does illustrate to what extent on-board optical measurements can reduce the a posteriori uncertainties in camera pointing.

1b) It may be possible to reduce by as much as a factor of 10 (Cases 1 and 2) the current uncertainties in satellite mass, often quoted as 10% for Io and Titan and 50 - 75% for Iapetus (de Sitter, 1931; Jeffreys, 1953; Kozai, 1957). Since the

satellite mass is estimated from the perturbing effect on the spacecraft, the mass estimate will depend rather strongly on the flyby distance to the satellite.

1c) An attempt to solve for the mass μ_0 of Jupiter failed because of very strong correlations with the mass and velocity of Io. While J_2 of Jupiter (Case 1b) could be determined to $\pm 14\%$, this cannot compete with the 1% uncertainty that de Sitter (1931) obtained by analyzing the motions of the Galilean satellites. The addition of J_3 and J_4 to Case 1b gave uncertainties of almost 100% in these parameters. In view of these negative results, no attempts were made to solve for the μ_0, J_2, J_3, and J_4 of Saturn.

2) It is highly desirable to extend the observations past the encounters with the satellite and its primary. Not only will this increase the total length of observing time, during which the satellite orbit will be seen under widely different viewing angles; but also it becomes possible to exploit the pronounced bending of the spacecraft's trajectory during the two encounters. We have seen that the bending caused by the satellite can reveal a surprisingly accurate value of its mass. Although a close passage of the satellite is required for a strong determination of mass, it is not mandatory that the satellite be observed during close-up (compare Cases 1 and 2 for Titan). For the improvement of satellite ephemerides, it is not even important that the spacecraft should come very close to the satellite. As long as their minimum range is not decreased (Cases 1 and 2 for Iapetus), it appears that relatively little is gained by concentrating the observations around the time of encounter. On the other hand, it is probably not worthwhile to include observations that are much farther removed than 30 days from encounter. At $E \pm 30^d$, an imaging resolution of 10" would correspond to Earth-based resolutions of 0.5" at Jupiter and 0.25" at Saturn.

Acknowledgments

This study was undertaken in support of the activities of the Outer Planets Grand Tours Imaging Science Team, of which the author was a member. The author wishes to thank the other members, in particular the team leader, Dr. M.J.S. Belton, for many valuable suggestions and criticisms. Thanks are also due to several JPL staff

members: the team's experiment representative, Mr. S.A. Collins, Mr. L.L. Simmons, and Dr. P.A. Penzo. The last provided the necessary MJS trajectory information.

The author gratefully acknowledges the financial support under NASA Grant NGR 09-015-184 and JPL contract BF-571747.

References

Aksnes, K.: 1972, Astron. and Astrophys. 17, 70.

Born, G. and Duxbury, T.: 1972, Abstract from AAS Division of Planetary Sciences meeting, submitted to Bull. Am. Astron. Soc., Feb. 25.

Burke, R.D., Miles, R.F., Penzo, P.A., Van Dillen, F.L., and Wallace, R.A.: 1972, paper to be presented at the AAS-AIAA Astrodyn. Conf. at Palo Alto, Calif., Sept. 11-13.

de Sitter, W.: 1931, Mon. Not. Roy. Astron. Soc., 91, 706.

Jeffreys, H.: 1953, Mon. Not. Roy. Astron. Soc., 113, 81.

Kozai, Y.: 1957/58, Annals of Tokyo Astron. Obs., 2nd series, 5, 73.

Table I

Distribution of Observations

Flyby	Number of observations	Observation interval	Comments
		Jupiter/Io (JST 77)	
			E = April 16.90 1979
			Δ_{Jup} = 420,200 km at E + 0^d
			Δ_{Io} = 41,300 km at E + 1.8^h
Case 1	20	E - 5^d to E - 0.5^d	
	41	E - 0.5 to E + 0.5	Δ_{Io} = 41,400 km at E + 1.7^h
	20	E + 0.5 to E + 5	
Case 2	124	E -30 to E +30	Δ_{Io} = 435,000 km at E - 11.1^h
		Saturn/Titan (JST 77)	
			E = Feb. 16.61 1981
			Δ_{Sat} = 138,400 km at E + 0^d
			Δ_{Ti} = 13,100 km at E - 19.0^h
Case 1	20	E - 5 to E - 1	
	61	E - 1 to E + 0.5	Δ_{Ti} = 14,200 km at E - 18.9^h
	20	E + 0.5 to E + 5	
Case 2	123	E -30 to E +30	Δ_{Ti} = 1,200,000 km at E - $1^d 14.9^h$
Case 3	60	E -30 to E - 1.5	
Case 4	55	E -30 to E - 4	Δ_{Ti} = 4,890,000 km at E - $3^d 22.4^h$
		Saturn/Iapetus (JSI 77)	
			E = May 4.70 1981
			Δ_{Sat} = 192,700 km at E + 0^d
			Δ_{Ia} = 7,400 km at E + $2^d 21.4^h$
Case 1	40	E -30 to E - 0.5	
	58	E - 0.5 to E + 6.5	Δ_{Ia} = 133,000 km at E + $2^d 18.7^h$
	34	E + 6.5 to E +30	
Case 2	126	E -30 to E +30	
Case 3	68	E -30 to E + 2	Δ_{Ia} = 941,000 km at E + $2^d 2.0^h$
Case 4	63	E -30 to E + 0	Δ_{Ia} = 4,020,000 km at E - 5.6^h

Table II

Standard Errors (line 1) and Actual Errors (line 2)

Flyby	σx_{10}	σy_{10}	σz_{10}	$\sigma \dot{x}_{10}$	$\sigma \dot{y}_{10}$	$\sigma \dot{z}_{10}$	σx_{20}	σy_{20}	σz_{20}	$\sigma \dot{x}_{20}$	$\sigma \dot{y}_{20}$	$\sigma \dot{z}_{20}$	$\sigma \mu_2$	σJ_2	Epoch
		(km)			(m/sec)			(km)			(m/sec)			(%)	
Jupiter/Io															
Case 1a	12	7	4	0.33	0.23	0.17	12	7	4	0.34	0.25	0.16	0.8		$E+0^d$
	4	3	3	0.16	0.06	0.16	4	3	3	0.12	0.01	0.18	0.3		
Case 1b	13	23	4	0.45	0.33	0.26	13	22	4	0.51	0.28	0.21	1.4	14.0	$E+0^d$
	3	7	3	0.11	0.10	0.13	3	6	3	0.06	0.03	0.16	0.1	2.4	
Case 2	38	23	5	0.77	0.92	0.36	68	32	22	1.03	1.50	0.41	2.6		$E+0^d$
	32	31	1	0.30	1.16	0.24	35	23	6	0.30	1.47	0.02	0.6		
Saturn/Titan															
Case 1	13	20	15	1.64	1.45	1.69	17	65	26	0.55	0.35	0.43	0.1		$E+0^d$
	4	15	11	1.10	0.37	1.26	8	25	12	0.16	0.16	0.09	0.1		
Case 2	6	106	41	5.04	1.98	6.24	37	38	33	0.17	0.13	0.20	1.4		$E+0^d$
	2	51	25	2.50	0.32	3.38	53	64	29	0.27	0.09	0.20	0.4		
Case 3a	53	442	68	0.87	0.76	0.14									$E-19.0^h$
	27	99	11	0.71	0.76	0.91									
Case 3b	632	2443	388	4.51	3.55	0.36	522	166	59	1.12	2.08	0.33			$E-19.0^h$
	205	159	105	0.52	1.79	0.53	103	147	101	0.35	0.54	0.59			
Case 3c							51	101	35	0.50	0.21	0.25			$E-19.0^h$
							14	26	54	0.16	0.02	0.58			
Case 4							255	125	83	0.65	1.01	0.31			$E-19.0^h$
							39	107	211	0.51	0.06	0.23			
Saturn/Iapetus															
Case 1	20	82	19	3.61	1.94	0.40	122	151	32	0.36	0.28	0.21	4.3		$E+0^d$
	1	49	13	2.36	0.18	0.15	8	10	5	0.03	0.26	0.03	0.5		
Case 2	41	144	35	6.35	2.41	0.45	139	168	36	0.40	0.25	0.21	9.1		$E+0^d$
	15	58	10	2.63	2.39	0.09	119	200	30	0.38	0.11	0.09	8.7		
Case 3a	93	173	45	0.18	0.51	0.15									$E+2^d21.4^h$
	64	128	27	0.05	0.17	0.01									
Case 3b	1159	2042	479	4.12	9.98	2.27	1592	2635	593	1.18	3.49	0.94			$E+2^d21.4^h$
	1465	2297	638	5.58	12.00	3.15	2008	3219	778	0.44	4.52	1.04			
Case 3c							91	144	35	0.15	0.21	0.09			$E+2^d21.4^h$
							100	150	43	0.17	0.14	0.03			
Case 4							95	324	91	0.18	0.43	0.13			$E+2^d21.4^h$
							27	84	108	0.05	0.17	0.11			

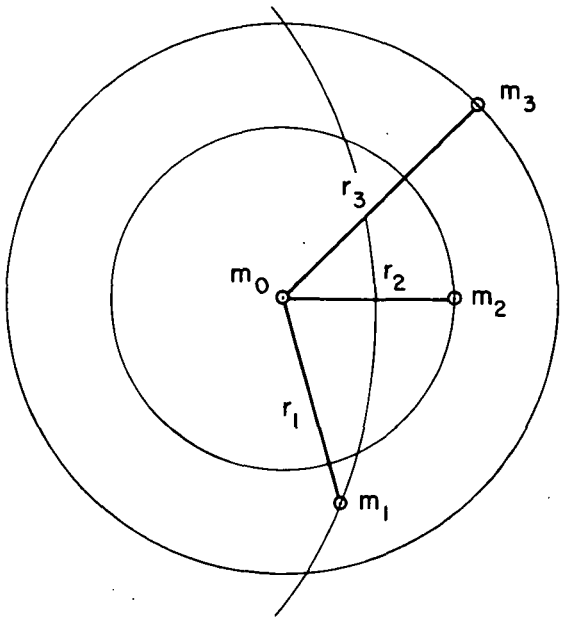

Fig. 1. MJS flyby geometry.